

UDC 532.517:537.584

SHELL MODELS IN RAPIDLY ROTATING DYNAMO SYSTEMS

M. Reshetnyak¹ and B. Steffen²

A typical feature of convection of rapidly rotating planets is a geostrophic state. This state is characterized by the following two different scales: the large one along the axis of rotation and the small transverse one. For the liquid cores of planets, their ratio can be some orders of magnitude already at the onset of convection. This phenomenon complicates simulations of convection and dynamo processes and requires a special analysis, essentially in the nonlinear regime. We consider the main features of the spectra for various intensities of heat sources in the existing spherical models of convection and geodynamo and propose a simple shell model which can mimic some properties of the original dynamo system.

1. Introduction. The last decade saw some fascinating progress in the modeling of the planetary dynamo, the Earth's dynamo in particular. While some years ago the main question was whether the heating from below in the simple Boussinesq system of a rotating sphere can sustain the selfgenerating magnetic field, now there are a variety of models which, at least at large-scales, provide a reasonable behavior of a magnetic field comparable with observations [1]. As it usually happens in astrophysical bodies, the convection and the magnetic field generation take place at a very wide range of scales. So, using commonly accepted estimates of the Reynolds number ($Re \sim 10^9$), the Prandtl number ($Pr \sim 10^8$) for the Earth's liquid core, for the 3D geometry one immediately obtains an estimate for the number of degrees of freedom of order $\sim Re^{9/4} \sim 10^{20}$, which for sure is out of reach of any modern computer for foreseeable time. The situation with direct numerical simulations (DNS) of a magnetic field is not so dramatic, since $R_m \sim 10^3$, but even this simulation is at the level of the modern computer's capacity. So, the DNS cannot handle the desired range of parameters and one should switch to different methods.

Usually, in many physical and technical problems the large eddy simulations (LES) is a good choice. This approach provides a description of the effective influence of the fields at subgrid scales on the large-scale fields. There is a number of papers on this subject, starting from the rigorous renormalization group analysis [2] to the simple but robust Prandtl and Smagorinsky models [3]. At least in principle, this approach allows one to provide a dynamic (in time) inhomogeneous (in space) distribution of turbulent coefficients for use in the original partial differential equations (PDE). By now, however, practically all the papers on the geodynamo are based on the assumption that the turbulent coefficients are constant parameters in time and space. Their particular values are defined by the numerical resolution available in the model [4]. This strange feature of geodynamo models has a deep background. As we know, without any exception all the planets of the solar system which have their own magnetic field due to the dynamo process belong to the so-called class of rapidly rotating bodies, where the ratio of the solar day τ_{sd} ($\tau_{sd} \sim \Omega^{-1}$, where Ω is the daily angular velocity of the body) to the typical convective time $\tau_c \sim \frac{l}{v}$ (v and l are the typical velocity and scale) is extremely small (the Rossby number $Ro = \frac{\tau_{sd}}{\tau_c} \ll 1$).

From the early theoretical works of Chandrasekhar summarized in [5] it follows that in the presence of rapid rotation the thermal convection degenerates to a quasi-two-dimensional form with small gradients of the fields along the axis of rotation and with large gradients in the perpendicular directions. As a result, the kinetic energy maximum occurs at very small scales. For the full dynamo problem with a magnetic field, at least for the moderate modified Rayleigh numbers Ra (in units [6, 7] of its critical value for a given Ekman number E), the situation is similar: the position of the maximum of the magnetic and kinetic spectra is very close to the estimate for the leading mode, so that the critical azimuthal wavenumber $m_{cr} \sim E^{-1/3}$ [8, 9]. On the other hand, such a coincidence cannot be expected for the regimes where the magnetic diffusion is much stronger than the viscous dissipation and the magnetic spectrum is shorter than the kinetic energy spectrum, as it is believed to be in the planets.

¹ Institute of the Physics of the Earth, Russian Academy of Sciences, 123995 Moscow, Russian Federation; e-mail: reshetnyak@ifz.ru; Research Computing Center of Moscow State University, 119992, Moscow, Russian Federation; e-mail: rm@uipe.srcc.msu.su

² Central Institute for Applied Mathematics (ZAM) of Forschungszentrum Jülich, D-52425, Jülich, Germany; e-mail: b.steffen@fz-juelich.de

Calculations with higher Ra , close to the ones in the Earth's core, show that the spectrum is nearly flat up to m_{cr} and then breaks. The well-known fact that the spectrum of the observed geomagnetic field decays as $\sim e^{-0.1m}$ [10] gives information on the poloidal part of the field at the surface of the core only. At the same time, the contribution of small scale fields in the bulk of the core can be already quite considerable, at least in the directions perpendicular to the rotation axis. The simple estimate of m_{cr} for the Earth's core with $E = 10^{-15}$ gives $m_{cr} \sim 10^5$. This means that already at the onset of thermal convection the DNS cannot be used. At the same time, the application of an isotropic and homogeneous semiempirical turbulence model (like Kolmogorov's one) is not suitable for the description of the geostrophic quasi-two-dimensional turbulence in the limit of $E \rightarrow 0$. Below we describe the dynamo equations in terms of the shell models. This approach has been well developed for the analysis of the isotropic turbulence and provided spectral properties of the stochastic fields for $Re \gg 1$ [11]. We propose its extension to quasi-geostrophic flows. The model developed is a toy model and can mimic only a few properties of the MHD systems: the energy exchange between the different components of the fields, the transition of heat energy to the kinetic energy and then to the magnetic energy, an increase of the critical modified Rayleigh number due to the rapid rotation ($\sim E^{-1/3}$), and the flat behavior of the spectrum for $m < m_{cr}$, comparable with that in geodynamo DNS.

2. Basic equations and linear analysis. The geodynamo equations for an incompressible fluid ($\nabla \cdot \mathbf{V} = 0$) in a volume of scale L rotating with an angular velocity Ω in the Cartesian coordinate system (x, y, z) in its traditional dimensionless form can be written as follows:

$$\begin{aligned} \frac{\partial \mathbf{B}}{\partial t} &= \nabla \times (\mathbf{V} \times \mathbf{B}) + q^{-1} \Delta \mathbf{B}, \\ E \text{ Pr}^{-1} \left[\frac{\partial \mathbf{V}}{\partial t} + (\mathbf{V} \cdot \nabla) \mathbf{V} \right] &= -\nabla P - \mathbf{1}_z \times \mathbf{V} + Ra T z \mathbf{1}_z + (\nabla \times \mathbf{B}) \times \mathbf{B} + E \Delta \mathbf{V}, \\ \frac{\partial T}{\partial t} + (\mathbf{V} \cdot \nabla)(T + T_0) &= \Delta T. \end{aligned} \quad (1)$$

Here the velocity \mathbf{V} , the magnetic field \mathbf{B} , the pressure P , and the typical diffusion time t are measured in the units of $\frac{\kappa}{L}$, $\sqrt{2\Omega\kappa\mu\rho}$, $\frac{\rho\kappa^2}{L^2}$, and $\frac{L^2}{\kappa}$, respectively, where κ is the thermal diffusivity, ρ is the density, μ is permeability, $\text{Pr} = \frac{\nu}{\kappa}$ is the Prandtl number, $E = \frac{\nu}{2\Omega L^2}$ is the Ekman number, ν is the kinematic viscosity, η is the magnetic diffusivity, $q = \frac{\kappa}{\eta}$ is the Roberts number, $Ra = \frac{\alpha g_0 \delta T L}{2\Omega\kappa}$ is the modified Rayleigh number, α is the coefficient of volume expansion, δT is the unit of temperature (for more details see [4]), and g_0 is the gravitational acceleration. In the case of magnetoconvection, the modified Elsasser number Λ appears (it describes the amplitude of the imposed magnetic field \mathbf{B}_0): $\Lambda = \frac{B_0^2}{\mu\rho\eta\Omega}$ Pr , where the first multiplier is the Elsasser number in its traditional form. Note that T_0 describes external heating.

Now we are looking for the linear solution Θ , $\mathbf{V} = (U_x, U_y, U_z)$, $\mathbf{B} = (B_x, B_y, B_z)$ with the imposed magnetic field $\mathbf{B}_0 = (0, 0, B_0)$, neglecting all small quadratic nonlinear terms. The application of the curl and double curl operators to the Navier-Stokes equation and the curl operator to the induction equation yields:

$$\begin{aligned} \frac{\partial B_z}{\partial t} &= \frac{\partial U_z}{\partial z} + q^{-1} \nabla^2 B_z, \\ \frac{\partial J_z}{\partial t} &= \frac{\partial W_z}{\partial z} + q^{-1} \nabla^2 J_z, \\ E \text{ Pr}^{-1} \frac{\partial \nabla^2 U_z}{\partial t} &= E \nabla^4 U_z + Ra \Delta_1 T - \frac{\partial W_z}{\partial z} + \Lambda \nabla^2 \frac{\partial B_z}{\partial z}, \\ E \text{ Pr}^{-1} \frac{\partial W_z}{\partial t} &= E \nabla^2 W_z + \frac{\partial U_z}{\partial z} + \Lambda \frac{\partial J_z}{\partial z}, \\ \frac{\partial T}{\partial t} + U_z &= \Delta T, \end{aligned} \quad (2)$$

where $W_z = \text{rot}_z \mathbf{V}$, $\Delta_1 = \frac{\partial}{\partial x^2} + \frac{\partial}{\partial y^2}$, and $\frac{\partial T_0}{\partial z} = 1$. By definition, \mathbf{W} is the vorticity of the velocity field \mathbf{V} and $\mathbf{J} = \nabla \times \mathbf{B}$ is an electric current, $\nabla T_0 \equiv \frac{\partial T_0}{\partial z} = 1$. The substitution of $(B_z, J_z, U_z, W_z, T) =$

$(b_z, j_z, u_z, w_z, \theta)e^{\gamma t + i(k_x x + k_y y + k_z z)}$ into (2) leads to

$$\begin{aligned} \gamma b_z &= ik_z u_z - q^{-1} k^2 b_z, & \gamma j_z &= ik_z w_z - q^{-1} k^2 j_z, & \gamma \theta &= u_z - k^2 \theta, \\ -E \text{Pr}^{-1} \gamma k^2 u_z &= E k^4 u_z - \text{Ra} \theta k^2 - ik_z w_z - \Lambda ik_z k^2 b_z, & E \text{Pr}^{-1} \gamma w_z &= -E k^2 w_z + ik_z u_z - i \Lambda k_z j_z, \end{aligned} \quad (3)$$

where $2^{-1/2} k = k_x = k_y \gg k_z \sim 1$. From the continuity condition $v_i k_i = 0$ ($b_i k_i = 0$) it follows that $u_x \simeq -u_y$ ($b_x \simeq -b_y$). The relations (3) can be represented in matrix form as follows:

$$A \cdot (b_z, j_z, u_z, w_z, \theta)^T = 0, \quad (4)$$

where

$$A = \begin{pmatrix} \gamma + q^{-1} k^2 & 0 & -ik_z & 0 & 0 \\ 0 & \gamma + q^{-1} k^2 & 0 & -ik_z & 0 \\ i \Lambda k_z & 0 & -E (\text{Pr}^{-1} \gamma + k^2) & ik_z k^{-2} & \text{Ra} \\ 0 & i \Lambda k_z & -ik_z & E (\text{Pr}^{-1} \gamma + k^2) & 0 \\ 0 & 0 & -1 & 0 & \gamma + k^2 \end{pmatrix}. \quad (5)$$

The main results of a dispersion analysis of (3–5) can be found in [12]. In the purely thermal regime without rotation, we have $\text{Ra}_{\text{cr}} \sim \mathcal{O}(1)$ and $k_{\text{cr}} \sim \mathcal{O}(1)$. The effect of rotation leads to a decrease of the transverse scales, to an increase of dissipation, and, as a result, to an increase of the critical Rayleigh number: $\text{Ra}_{\text{cr}} \sim E^{-1/3}$ and $k_{\text{cr}} \sim E^{-1/3}$. Depending on a value of the Prandtl number, the first marginal mode can be either non-oscillating ($\text{Pr} > 1$), or oscillating ($\text{Pr} < 1$) with $\omega_{\text{cr}} \sim E^{-2/3}$. The magnetic field in the z -direction imposed alone without rotation leads to the same suppression of convection: $\text{Ra}_{\text{cr}} \sim \Lambda$ and $k_{\text{cr}} \sim \text{Ha}^{1/3}$, where the Hartman number is $\text{Ha} = (\Lambda E^{-1})^{1/2}$.

For the combined effects (rotation with an imposed magnetic field) and for the weak magnetic field state, one has $\text{Ra}_{\text{cr}} \sim E^{-1/3}$, when $\Lambda < E^{1/3}$ and $k_{\text{cr}} \sim \text{Ra}_{\text{cr}} \sim \mathcal{O}(1)$ for $\Lambda \sim \mathcal{O}(1)$, the so-called strong field regime. A later decrease of Ra_{cr} is a consequence of MHD instabilities which can occur when transition from the weak to strong regimes takes place. This corresponds to the case where both effects neutralize each other. The reverse scenario, when the arising small-scale turbulence damps the large-scale magnetic field generation, is known as the dynamo catastrophe (see a review of the problem in [4]). From the very beginning, it is clear that such an idealized model can only predict the possibility of instabilities, but cannot be a serious foundation for the far-reaching conclusions on the strong nonlinear regimes of MHD systems without checking it in DNS.

3. Experience from DNS. We classify results on the Boussinesq dynamo into two classes: the weak convection regime with $\text{Ra} \sim (1, \dots, 10) \text{Ra}_{\text{cr}}$ and the strongly convective regime with $\text{Ra} \sim (10^2, \dots, 10^3) \text{Ra}_{\text{cr}}$. The detailed statistics of various features of these regimes are presented in [4]. Further we will focus our attention on the spectral properties of the fields averaged over the bulk of the liquid core.

The typical behavior of the kinetic energy spectrum for $E = 10^{-5}$ without a magnetic field is presented in Figure 1a. These calculations are based on the control-volume model [13] in a rotating spherical shell for the problem (1) with a grid of 250^3 points. For low Rayleigh numbers, the maximum corresponds to the critical wavenumber $m_{\text{cr}} \sim 10^1$ predicted in linear analysis. A similar picture was observed in DNS by [6] and [7] in full dynamo models. The magnetic energy spectrum was very similar to the kinetic energy spectrum. So, as in the previous case, the maxima of these spectra agree with the prediction of linear analysis for the purely thermal convection. Convection at large-scales is too weak to start an efficient magnetic field generation at these scales and both maxima are localized at m_{cr} . This is the reason why the columnar structure of flow is not strongly disturbed by the magnetic field when the dynamo process is switched on.

An increase of the Rayleigh number destroys the regular columnar structure of flow and leads to a flattening of the spectrum at $m < m_{\text{cr}}$ (Figure 1b). This phenomenon is well observed in dynamo simulations discussed in [14], where the break in both the spectra for $E \sim 10^{-6}$ corresponds to $m_{\text{cr}} \sim 20$. The typical form of the spectrum is presented in Figure 1b. Below we consider the shell model technique, which helps to proceed to smaller values of E and to longer spectra. It would not be reasonable to expect that this approach will reproduce all the details for the weak turbulent flows for moderate Rayleigh numbers; however, it is a helpful tool when the fields are rescalable at the wider range of scales.

4. The dynamo shell models. The idea of the shell model approach is to mimic the original partial differential equations by a dynamical system with a system of ordinary differential equations. Usually, such an idea is implemented for the isotropic homogeneous turbulence, see review in [11]. Following the shell approach,

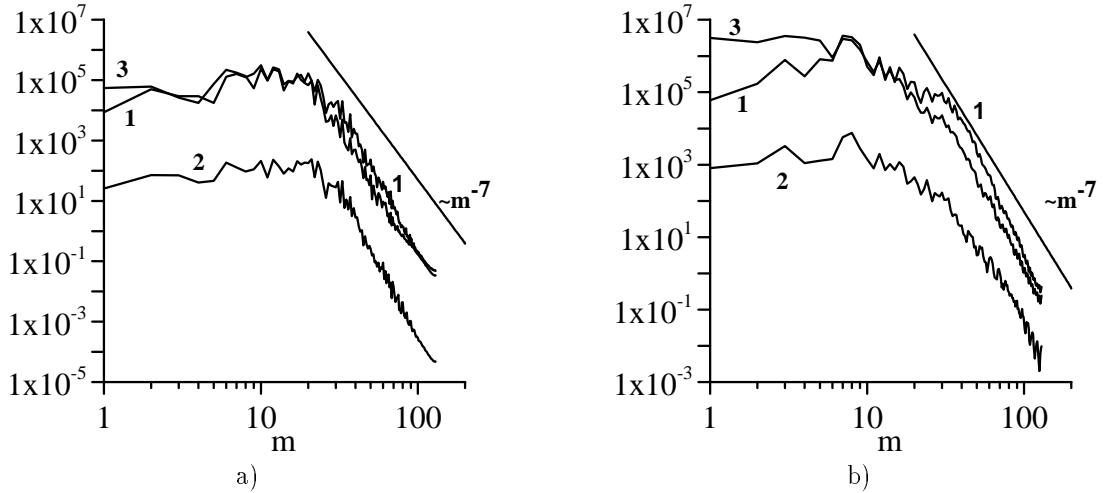


Fig. 1. The Fourier spectra in the azimuthal direction at the equatorial plane of V_r -components (1) , V_θ -components (2) and V_ϕ -components (3) of the velocity field for $E = 10^{-5}$, $Pr = 1$ and $Ra = 150$ (a), $Ra = 600$ (b) in the large-scale spherical model. The V_θ -component is antisymmetric relative to the equator plane and its amplitude is considerably smaller than the other two components

one has to write the equations in the Fourier space, making the two assumptions: only local (in k -space) interactions occur (e.g., the mode with wavenumber k is produced by harmonics with wavenumbers $k - 1$ and $k + 1$) and $k_n = \alpha k_{n-1}$ (with $k_0 = 1$), where α is a constant, usually $\alpha = 2$. This logarithmic distribution of the wave vectors makes it possible to cover a very large range of scales needed in the simulations. As an example, we present the most popular GOY shell model, named after the three authors of [15, 16]:

$$\frac{dU_n}{dt} = k_n \left(-\frac{1}{8} U_{n-2} U_{n-1} - \frac{1}{4} U_{n-1} U_{n+1} + U_{n+1} U_{n+2} \right) - \nu k_n^2 U_n \quad (6)$$

with $n = 0, \dots, n_{\max}$ and with the cut-off $n_{\max} \sim Re^{3/4}$. Since this model was developed under the assumption of isotropy for the velocity field U , there is no Coriolis force in (6). In spite of the apparently simple form of (6), this model satisfies the two conservation laws of the original Navier–Stokes equation: the conservation of the kinetic energy \mathcal{E} and of the hydrodynamic helicity \mathcal{H} in the limit of vanishing viscosity ν :

$$\mathcal{E} = \sum_n |U_n|^2, \quad \mathcal{H} = \sum_n (-1)^n k_n |U_n|^2. \quad (7)$$

The integration of (6) in time can be done for the very large Reynolds numbers of astrophysical applications, say $Re \sim 10^{10} - 10^{14}$, and gives reasonable scaling laws for turbulent flows [11].

Though the decomposition of the nonlinear terms accepted in the framework of the shell models is not unique in a strict mathematical sense, this approach was very fruitful for the modeling of the classical Kolmogorov’s-like turbulence. In this kind of turbulence, energy propagates through the spectrum in a “continuous” way: from one scale to the next closest one. For the Navier–Stokes equation and the heat flux equation in three dimensions, the energy transfer takes place from the large scales to the small ones (the direct cascade).

The next crucial contribution for our modeling was made by the authors of [17, 18] who solved the Boussinesq problem (the Navier–Stokes equation in the form (6) but with an Archimedean force $\sim Ra \theta_n$) and the shell equation for the temperature θ . The ideas of the truncated Fourier series used in the shell models were successfully applied to the dynamo equations (the Navier–Stokes equation and the induction equation combined), see [19]. The main point of this model is to provide the conservation of the total energy (the sum of the kinetic and magnetic energies) as well as the conservation of the cross helicity in the system. Using these components, the combined dynamo shell model for the isotropic homogeneous turbulence was presented in [20]. Note that the shell models can also be used for the description of subgrid fields and eddy diffusion in the control-volume models of the large-scale thermal convection [21].

However, the isotropic shell models can hardly be used for the modeling of the quasi-geostrophic (or magnetostrophic) turbulence, which is believed to be in the liquid core [22, 23]. As follows from Section 2, the rapid rotation (as well as the strong magnetic field) leads to the two-dimensionalization of the flow, so

that the two quite different scales can exist even at the threshold of magnetic field generation: the large scale along the axis of rotation (or in the direction of the imposed magnetic field B_z) and the small scale in the perpendicular plane. There is a possibility of a third scale along the strong azimuthal magnetic field [22] which we do not consider here. This is our motivation to build a two-dimensional shell model. Such a model was first given in [24] for the thermal convection equation without a magnetic field. Here we will use it as a part of the full dynamo model, so we recall some basic points. We consider an extension of the linear system (2) to the nonlinear regime, using a quasi-geostrophic approximation where it is needed. All the fields are represented by their two-dimensional Fourier modes, where the second index corresponds to the z -direction along the axis of rotation and the first one corresponds to the perpendicular x -direction. The corresponding wavenumbers are k_z and k_x . We start from the linear set of equations (3), rewrite it for the velocity and magnetic fields (instead of the vorticity \mathbf{w} and the electric current \mathbf{j}), and add nonlinear terms. The full system of equations for the magnetic field \mathbf{b} ($a = b_x$, $b = b_z$), the velocity field \mathbf{u} ($u = v_x$, $w = v_z$), and the temperature θ are proposed in the form

$$\begin{aligned}
 \frac{da_{ij}}{dt} &= i\varepsilon k_{xj} \left(u_{i+1,j}^* a_{i+2,j}^* + u_{i-1,j}^* a_{i+1,j}^* - \frac{u_{i-2,j}^* a_{i-1,j}^*}{2} + u_{i+2,j}^* a_{i+1,j}^* - \frac{u_{i+1,j}^* a_{i-1,j}^*}{2} - \frac{u_{i-1,j}^* a_{i-2,j}^*}{4} \right) \\
 &\quad + ik_{zj} \left(w_{i,j+1}^* a_{i,j+2}^* + w_{i,j-1}^* a_{i,j+1}^* - \frac{w_{i,j-2}^* a_{i,j-1}^*}{2} + w_{i,j+2}^* a_{i,j+1}^* - \frac{w_{i,j+1}^* a_{i,j-1}^*}{2} \right. \\
 &\quad \left. - \frac{w_{i,j-1}^* a_{i,j-2}^*}{4} \right) - ik_{zj} u_{ij}^* (b_{ij}^* + b_{i,j-1}^* + b_{i,j-2}^* + b_{i,j+1}^* + b_{i,j+2}^*) - q^{-1} (k_{xi}^2 + k_{zj}^2) a_{ij}, \\
 \frac{db_{ij}}{dt} &= i\varepsilon k_{xj} \left(u_{i+1,j}^* b_{i+2,j}^* + u_{i-1,j}^* b_{i+1,j}^* - \frac{u_{i-2,j}^* b_{i-1,j}^*}{2} + u_{i+2,j}^* b_{i+1,j}^* - \frac{u_{i+1,j}^* b_{i-1,j}^*}{2} - \frac{u_{i-1,j}^* b_{i-2,j}^*}{4} \right) \\
 &\quad + ik_{zj} \left(w_{i,j+1}^* b_{i,j+2}^* + w_{i,j-1}^* b_{i,j+1}^* - \frac{w_{i,j-2}^* b_{i,j-1}^*}{2} + w_{i,j+2}^* b_{i,j+1}^* - \frac{w_{i,j+1}^* b_{i,j-1}^*}{2} - \frac{w_{i,j-1}^* b_{i,j-2}^*}{4} \right) \\
 &\quad - i\varepsilon k_{xi} w_{ij}^* (a_{ij}^* + a_{i-1,j}^* + a_{i-2,j}^* + a_{i+1,j}^* + a_{i+2,j}^*) - q^{-1} (k_{xi}^2 + k_{zj}^2) b_{ij}, \\
 \frac{d\theta_{ij}}{dt} &= i\varepsilon k_{xj} \left(u_{i+1,j}^* \theta_{i+2,j}^* + u_{i-1,j}^* \theta_{i+1,j}^* - \frac{u_{i-2,j}^* \theta_{i-1,j}^*}{2} + u_{i+2,j}^* \theta_{i+1,j}^* - \frac{u_{i+1,j}^* \theta_{i-1,j}^*}{2} - \frac{u_{i-1,j}^* \theta_{i-2,j}^*}{4} \right) \\
 &\quad + ik_{zj} \left(w_{i,j+1}^* \theta_{i,j+2}^* + w_{i,j-1}^* \theta_{i,j+1}^* - \frac{w_{i,j-2}^* \theta_{i,j-1}^*}{2} + w_{i,j+2}^* \theta_{i,j+1}^* - \frac{w_{i,j+1}^* \theta_{i,j-1}^*}{2} \right. \\
 &\quad \left. - \frac{w_{i,j-1}^* \theta_{i,j-2}^*}{4} \right) - (k_{xi}^2 + k_{zj}^2) \theta_{ij} + w_{ij}, \\
 2 \text{Pr}^{-1} \text{E} \frac{du_{ij}}{dt} &= 2 \text{Pr}^{-1} \text{E} i \left[\varepsilon k_{xi} \left(u_{i+1,j}^* u_{i+2,j}^* - \frac{u_{i-1,j}^* u_{i+1,j}^*}{4} - \frac{u_{i-2,j}^* u_{i-1,j}^*}{8} \right) \right. \\
 &\quad \left. + k_{zj} \left(\frac{u_{i,j-1}^* w_{ij}^*}{2} + 2u_{i,j+1}^* w_{ij}^* \right) - \varepsilon k_{xi} \left(\frac{w_{i-1,j}^* w_{ij}^*}{2} + 2w_{i+1,j}^* w_{ij}^* \right) \right] \\
 &\quad - 2\text{E} (k_{xi}^2 + k_{zj}^2) u_{ij} - w_{ij} \frac{k_{zj}}{k_{xi}} - ik_{zj} a_{ij}^* (b_{ij}^* + b_{i,j-2}^* + b_{i,j-1}^* + b_{i,j+1}^* + b_{i,j+2}^*), \\
 \text{Pr}^{-1} \text{E} \frac{dw_{ij}}{dt} &= \text{Pr}^{-1} \text{E} i \left[k_{zj} \left(w_{i,j+1}^* w_{i,j+2}^* - \frac{w_{i,j-1}^* w_{i,j+1}^*}{4} - \frac{w_{i,j-2}^* w_{i,j-1}^*}{8} \right) \right. \\
 &\quad \left. + 2\varepsilon k_{xi} \left(\frac{w_{i-1,j}^* u_{ij}^*}{2} + 2w_{i+1,j}^* u_{ij}^* \right) - 2k_{zj} \left(\frac{u_{i,j-1}^* u_{ij}^*}{2} + 2u_{i,j+1}^* u_{ij}^* \right) \right] \\
 &\quad - \text{E} (k_{xi}^2 + k_{zj}^2) w_{ij} + u_{ij} \frac{k_{zj}}{k_{xi}} + \text{Ra} \theta_{ij} - i\varepsilon k_{xi} b_{ij}^* (a_{i-2,j}^* + a_{i-1,j}^* + a_{ij}^* + a_{i+1,j}^* + a_{i+2,j}^*).
 \end{aligned} \tag{8}$$

The form of the nonlinear terms in the heat flux equation is adopted from the one-dimensional model [18] and ε is 1 or $\text{E}^{1/3}$, depending on the convection regime. This form of the discrete operator provides the conservation of the heat energy $\sim \theta^2$ in the limit of vanishing thermal diffusion. The only energy source in this system is described by the last term in the right-hand side of the equation.

As regards to the convective and magnetic parts, we stress the following points. In both the equations

for the velocity and the magnetic field we take into account only one conservation law: the conservation of energy. Here we do not consider the helicity conservation and the cross helicity conservation (at least, not all the chains in (8) provide the conservation of these integrals). This makes our model simpler and we hope to take into account these effects in the future. Note that at least for the three dimensional case, the spectral characteristics do not change much when one considers either the GOY model with the conservation of energy and helicity together, or the simpler model [25] with the only one integral, the kinetic energy. Note also that the helicity conservation $h \sim v_z w_z$ in a rapidly rotating body, where both the multipliers are defined at very different scales, is in principle impossible in terms of the one-dimensional shell model with local interactions in the k -space only [26].

To construct shell equations for the velocity and magnetic fields, we “uncurl” equations for w_z and j_z in (3) and rewrite them for the x -component of the fields, adding the nonlinear terms and assuming that $w \sim ik_x u$ and $j \sim ik_x a$. For the isotropic convection without the Coriolis force, we have to get two similar equations which should reproduce properties of the fields similar to the one-dimensional shell model, see (8) with $\varepsilon = 1$.

This set of equations (8) provides the conservation of kinetic and magnetic energies in the limit of zero diffusion, the exchange of kinetic and magnetic energies, and the feedback of the magnetic field on the flow. In Figure 2 we present simulations for the regimes without rotation, $\varepsilon = 1$. The slight asymmetry of the x - and z -components of the spectrum is due to the fact that the Archimedean force in the system has only the z -component. All the spectra have the Kraichnan–Iroshnikov slope $-3/2$ [27, 28]. We call to attention that this regime mimics the full dynamo model (1) with a prescribed heat source energy (T_0) at $n = 0$ and with the equipartition state when the kinetic and magnetic energies $\frac{V^2}{2}$ and $\frac{\text{Pr} B^2}{2E}$ are of the same order of magnitude.

The next step is to take into account rotation. This means that in the limit of rapid rotation our model should imitate the geostrophic or magnetostrophic regime. The point is that even for the fully developed turbulence, when $\text{Re} \sim 10^9$, the convective term for the Navier–Stokes equation in the Earth’s core is much less than the Coriolis term. Basing on the dominant scale of the core and the west drift velocity, one has that this difference is of three orders of magnitude. In the zero order, hence, there is a geostrophic balance (the balance of the Coriolis force and the pressure) or a magnetostrophic balance when the Lorentz force is taken into account. Note that because $\frac{\text{Pe}}{\text{R}_m} = \text{q}^{-1} \sim 10^5$ is quite large and the spectrum of the magnetic field generated should be shorter than the convective one, the two forms of the balance can exist at different scales. Then, for a description of turbulence we need to exclude the large terms from the equations and retain only the terms which will be of order of convective ones. (Otherwise, the Coriolis force blocks the energy transfer in the shell model and the spectrum collapses.) The main features of the geostrophic balance are that $w_z \sim 2ik_x u_x$ and $|k_x u_x| \sim -|k_y u_y| \gg |k_z u_z|$ (similar for j and a). This means that the convective transport of a quantity in the transverse direction will be proportional to k_z , but not to k_x . The physical nature of this phenomenon is trivial. In spite of the strong gradients of the fields, which would provide an intensive convective flux in the case without rotation, rotation leads to a swirling of the flow and damps fluxes in the transverse directions. This mechanism is well-observed in the different thermal regimes in the Taylor cylinder (where rotation does not prevent a heat flux in z -direction) and outside the cylinder, where the convective thermal flux is blocked by the Coriolis force [29]. That is why we put $\varepsilon = E^{1/3}$ when we come to the geostrophic state: $|k_x u| \gg |k_z v|$. This trick blocks the direct cascade to the high wavenumbers in x -direction and leads to the flattening of the spectra. We emphasize that because we started from (3)–(5), our shell model is able to reproduce features of the system (2) known from linear analysis (see Section 2).

In Figure 3 we present the dynamo simulations for large and small Roberts numbers q , which can change the length of the magnetic spectra and, more important, the location of the magnetic spectra relative to the break of the convective spectra at $\sim m_{\text{cr}}$. In both the cases, we observe a flat behavior of the fields for wavenumbers

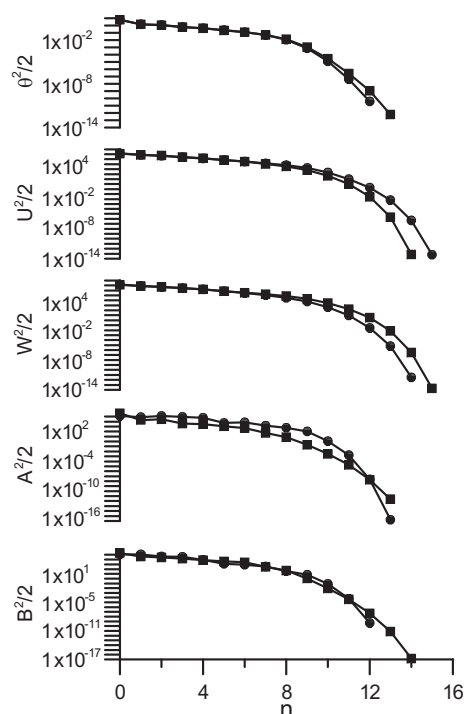


Fig. 2. Spectra of the fields for the shell dynamo problem (8) without Coriolis force, $E = 10^{-4}$, $\text{Ra} = 1.3 \cdot 10^3$, $\text{Pr} = \text{q} = 0.1$. Squares correspond to the z -spectrum and circles to the x -spectrum

In spite of the strong gradients of the fields, which would provide an intensive convective flux in the case without rotation, rotation leads to a swirling of the flow and damps fluxes in the transverse directions. This mechanism is well-observed in the different thermal regimes in the Taylor cylinder (where rotation does not prevent a heat flux in z -direction) and outside the cylinder, where the convective thermal flux is blocked by the Coriolis force [29]. That is why we put $\varepsilon = E^{1/3}$ when we come to the geostrophic state: $|k_x u| \gg |k_z v|$. This trick blocks the direct cascade to the high wavenumbers in x -direction and leads to the flattening of the spectra. We emphasize that because we started from (3)–(5), our shell model is able to reproduce features of the system (2) known from linear analysis (see Section 2).

In Figure 3 we present the dynamo simulations for large and small Roberts numbers q , which can change the length of the magnetic spectra and, more important, the location of the magnetic spectra relative to the break of the convective spectra at $\sim m_{\text{cr}}$. In both the cases, we observe a flat behavior of the fields for wavenumbers

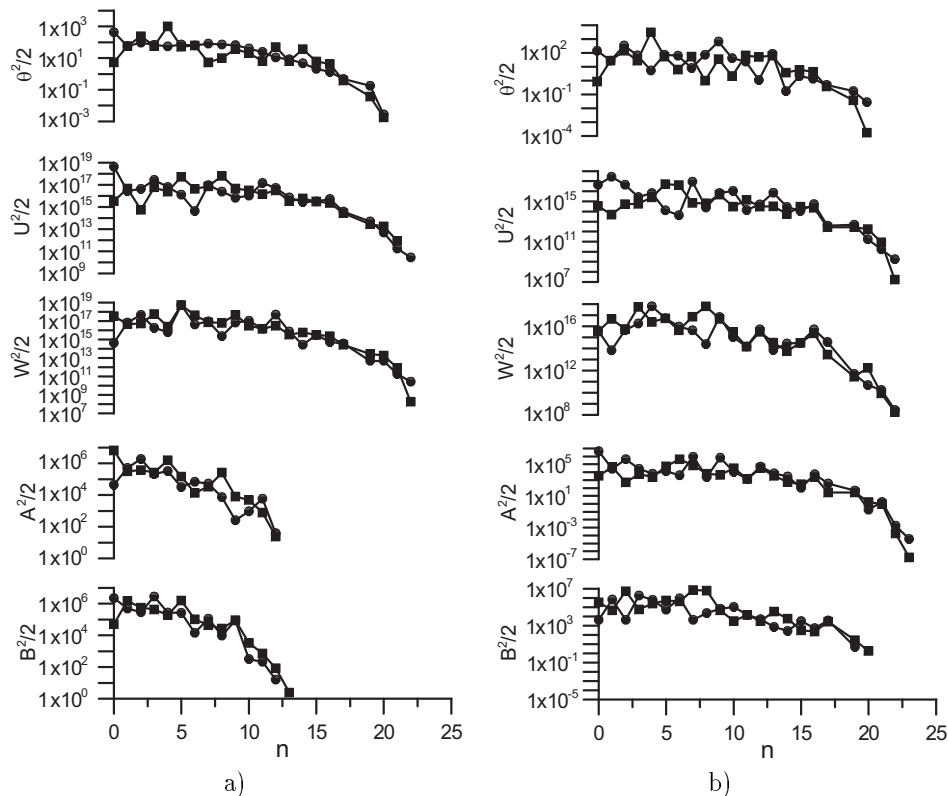


Fig. 3. Spectra of the fields for the dynamo problem (8) with Coriolis force, $E = 10^{-10}$, $Ra = 1.8 \cdot 10^4$, $Pr = 0.1$, $q = 10^{-3}$ (a) and $q = 10^2$ (b). Squares indicate the z -spectrum and circles the x -spectrum

up to $\sim m_{cr}$ with a subsequent decrease. Calculations including the Coriolis force show less stability than the nonrotating simulations, resulting in an irregular form of the spectra. Moreover, the rotation introduces its own (short) time scale and the approximation of the Coriolis force is local in the wave space. Experiments with different approximations of the nonlinear terms show that stability gets better when the number of the products in the chain increases. From this point of view, the effects of the Coriolis force should be very unstable.

The flat behavior of the spectra means that the diffusion in the system is estimated by $\sim m_{cr}^2 (\mathbf{u}^2, \mathbf{j}^2)$. This is the reason why the eddy viscosity should be increased by a factor of $E^{-1/3}$ and can be used in LES [30].

We also note that the flat part of the kinetic energy spectra has far-reaching consequences for the energy budget of the whole system, since the main contribution to the dissipation in the system is of order $\sim E^{1/3} u_0^2$, not $\sim E u_0^2$!

5. Discussion. We have considered a very important property of the rotating turbulence: the flattening of the spectra for the scales smaller than the diameter of the columns ($\sim E^{1/3}$). This flattening is caused by nonlinear interactions. Now, simple linear analysis reveals that the growth rate σ of the eigenmodes with realistic Ra for the small $k_x \sim 10^1$ is negative in the Earth's core [31]. Hence, the existing convection in this range of scales is due only to the nonlinear terms. The DNS of purely thermal convection and of the full dynamo problem demonstrates that already for the moderate values of Ra the kinetic energy distribution is flat for $m < m_{cr}$ and rapidly decays for larger m . So, since in the existing DNS the molecular diffusion coefficients are large, the magnetic spectrum obtained has a form similar to the kinetic one. To check what will happen for a small q and a kinetic energy spectrum long enough, one needs methods other than DNS, such that they help to resolve spectra with different lengths. With this end in view, we used the shell models. Our modeling shows that in this case the magnetic field is generated mainly at the large scales where the microscale Reynolds number $r_m = \frac{u_n}{k_n \eta}$ is sufficient for the magnetic field generation. Usually, the appearance of a magnetic field does not change the kinetic energy spectrum. This means that our nonlinear system comes to a stable state without the instabilities predicted in linear analysis. However, a further thorough analysis of the above-proposed model is required.

Acknowledgements. The first author is grateful to the Central Institute for Applied Mathematics (ZAM) of Forschungszentrum in Jülich for hospitality. This work was supported by the INTAS Foundation (grant № 03-51-5807) and by the Russian Foundation for Basic Research (grant № 06-05-64619a).

REFERENCES

1. *Kono M., Roberts P.* Recent geodynamo simulations and observations of the geomagnetic field // *Reviews of Geophysics*. 2002. **40**, N 10. B1–B41.
2. *McComb W.D.* The physics of fluid turbulence. Oxford: Clarendon Press, 1992.
3. *Monin A.S., Yaglom A.M.* Statistical fluid dynamics. NY: The MIT Press, 1971.
4. *Jones C.A.* Convection-driven geodynamo models // *Phil. Trans. R. Soc. London*. 2000. **A 358**. 873–897.
5. *Chandrasekhar S.* Hydrodynamics and hydromagnetic stability. NY: Dover Publications, 1981.
6. *Kutzner C., Cristensen U.R.* From stable dipolar towards reversing numerical dynamos // *Phys. Earth Planet. Inter.* 2002. **131**. 29–45.
7. *Simitov R.* Convection and magnetic field generation in rotating spherical fluid shells (Ph.D. Thesis). Bayreuth: University of Bayreuth, 2004.
8. *Roberts P.H.* On the thermal instability of a highly rotating fluid sphere // *Astrophys. J.* 1965. **141**. 240–250.
9. *Busse F.H.* Thermal instabilities in rapidly rotating systems // *J. Fluid Mech.* 1970. **44**. 441–460.
10. *Lowes F.J.* Spatial power spectrum of the main geomagnetic field // *Geophys. J. R. Astr. Soc.* 1974. **36**. 717–725.
11. *Bohr T., Jensen M., Paladin G., Vulpiani A.* Dynamical systems approach to turbulence. Cambridge: Cambridge University Press, 1998.
12. *Hollerbach R., Rüdiger R.* The magnetic Universe. Weinheim: Wiley-VCH Verlag GmbH & Co. KGaA, 2004.
13. *Reshetnyak M., Steffen B.* Dynamo model in the spherical shell // *Numerical Methods and Programming*. 2005. **6**, N 1. 32–38.
14. *Roberts P.H., Glatzmaier G.A.* A test on the frozen-flux approximation using a new geodynamo model // *Phil. Trans. R. Soc. Lond.* 2000. **A358**. 1109–1121.
15. *Gledzer E.B.* System of hydrodynamic type admitting two quadratic integrals of motion // *Sov. Phys. Dokl.* 1973. **18**, N 4. 216–225.
16. *Ohkitani K., Yamada M.* Temporal intermittency in the energy cascade process and local Lyapunov analysis in fully developed model turbulence // *Prog. Theor. Phys.* 1989. **81**, N 2. 329–334.
17. *Mingshun J., Shida L.* Scaling behavior of velocity and temperature in a shell model for thermal convective turbulence // *Physica Review E*. 1997. **56**, N 1. 441–446.
18. *Lozhkin S.A., Frick P.G.* Inertial Obukhov–Bolgiano interval in shell models of convective turbulence // *Fluid Dynamics* 1988. **33**, N 6. 125–140.
19. *Frick P., Sokoloff D.* Cascade and dynamo action in a shell model of magnetohydrodynamic turbulence // *Phys. Rev. E*. 1998. **57**. 4155–4164.
20. *Frick P., Reshetnyak M., Sokoloff D.* Cascade models of turbulence for the Earth's liquid core // *Doklady Earth Sciences*. 2002a. **387**, N 8. 988–991.
21. *Frick P., Reshetnyak M., Sokoloff D.* Combined grid-shell approach for convection in a rotating spherical layer // *Europhys. Lett.* 2002b. **59**, N 2. 212–217.
22. *Braginsky S.I., Meytlis V.P.* Local turbulence in the Earth's core // *Geophys. Astrophys. Fluid Dynamics*. 1990. **55**. 71–87.
23. *Matsushima M., Nakajima T., Roberts P.H.* The anisotropy of local turbulence in the Earth's core // *Earth Planets Space*. 1999. **51**. 277–286.
24. *Reshetnyak M.* The estimate of the turbulent viscosity of the Earth's liquid core // *Doklady Earth Sciences*. 2005a. **400**, N 1. 105–109.
25. *Desnianskii V.N., Novikov E.A.* Simulation of cascade processes in turbulent flows // *J. Appl. Math. Mech.* 1974. **38**. 507–513.
26. *Verma M.* Statistical theory of magnetohydrodynamic turbulence: recent results // *Phys. Reports*. 2004. **401**. 229–380.
27. *Iroshnikov P.S.* Turbulence of a conducting fluid in a strong magnetic field // *Sov. Astron.* 1964. **7**. 566–571.
28. *Kraichnan R.H.* Inertial-range spectrum of hydromagnetic turbulence // *Phys. Fluids*. 1965. **8**. 1385–1387.
29. *Glatzmaier G.A., Roberts P.H.* A three-dimensional convective dynamo solution with rotating and finitely conducting inner core and mantle // *Phys. Earth Planet. Inter.* 1995. **91**. 63–75.
30. *Reshetnyak M., Steffen B.* The subgrid problem of the thermal convection in the Earth's liquid core // *Numerical Methods and Programming*. 2004. **5**, N 1. 45–49.
31. *Reshetnyak M.* Dynamo catastrophe, or why the geomagnetic field is so long-lived // *Geomagnetism & Aeronomy*. 2005b. **45**, N 4. 571–575.

Received 11 February 2006